ANAS Transactions Earth Sciences 2 / 2024

http://www.journalesgia.com

THE USE OF GLOBAL GRAVITY FOR MAPPING THE RELATIONSHIP BETWEEN SEISMICITY AND GEOLOGIC STRUCTURE IN THE MIDDLE PART OF ACEH PROVINCE, INDONESIA

Yanis M.[1], Abdullah F.[1,2], Ananda R.[3], Syamsyudin F.[1,2], Ismail N.[1,2], Zainal M.[1], Paembonan A.Y.[4]

[1]Geophysical Engineering Department, Syiah Kuala University
Banda Aceh 23111, Indonesia: yanis@usk.ac.id
[2]Physics Department, Syiah Kuala University
Banda Aceh 23111, Indonesia
[3]Department of Geophysical Engineering, Bandung Institute of Technology
Bandung 40132, Indonesia
[4]Geophysical Engineering Department, Sumatra Institute of Technology
Lampung Selatan 35365, Indonesia

Keywords: *Gravity, fault, GGM+, Aceh Province, geological structure, 3D Inversion*

Summary. Aceh is one of the Indonesian provinces prone to earthquakes because it is traversed by the Great Sumatra Fault and the subduction zones along its west coast with high seismic activity. Recently, fault mapping research has focused on the Aceh and Seulimum segments in the western part of Aceh Province. In contrast, the central part has yet to be studied significantly, even though several earthquakes in the last 10 years have occurred in the areas where fault traces still need to be mapped properly. Therefore, this study used the global gravity model Plus (GGM+) with a high resolution of 200 m/px to analyze the relationship between seismicity and fault structures in the Central part of Aceh. The residual anomaly from GGM+ indicates that the existence of geological structures such as the Aceh, Pameu, and Samalanga segments are characterized by low gravity. Several derivative methods were also applied to clarify the existence of a fault, such as the horizontal derivative anomaly for mapping the Aceh, Batee, Samalanga, and Alue Lintang – Peusangan segments. The vertical derivative shows the existence of the Tringgadeng Fault, suspected as a source of the Pidie Jaya earthquake in 2016. Therefore, the tilt derivative can also visualize the presence of the Nissam fault, which is not shown in other filter methods. We also carried out a 3D gravity modelling using the Occam algorithm and Singular Value Decomposition (SVD); the density shows the fault structure's depth and geometry, generally 8 km, thus providing reliability of GGM+ in fault studies, especially in high elevation areas, which are challenging for instrument mobilization.

1. Introduction

The province of Aceh is traversed by the Great Sumatran Fault (GSF) line, which stretches ~1.900 km from Lampung to the Andaman Islands (McCaffrey, 2009; Hill et al., 2015). Seismicity data also shows that the southern part of Sumatra has experienced a lot of seismic activities, while the northern part has not released significant earthquakes for 170 years (Sieh and Natawidjaja, 2000). So, it is estimated that the Aceh Province has a potential for a big magnitude earthquake with Mw ≥ 7 if the stored energy in that area is released over a long period (Ito et al., 2012). This is a serious future threat to the Aceh region, considering that earthquakes on land are usually very harmful (Muksin et al., 2019). The GSF fault is divided into 19 segments, starting from the southernmost with a small strike-slip and increasing to the northern part of the island of Sumatra. Two earthquakes with a magnitude of Mw 7.7 occurred in 1936, and Mw 6.5 in 1964 caused severe damage around Banda Aceh (Fig.1), and another earthquake with a magnitude of Mw 9 in 2004 shocked Sumatra, followed by a tsunami (Lay et al., 2005). This event triggered aftershocks in the subduction zone and several segments of the GSF (Natawidjaja and Triyoso, 2007). Even though several researchers

have focused on the western part, Aceh and Seulimum Segments (Yanis et al., 2021b; Ghosal et al., 2012; Muksin et al., 2018). However, several recent earthquake events occurred at locations where the faults had not been mapped significantly, as shown in Figure 1. Significant seismic activity data from the USGS in the North Aceh region had a magnitude of Mw 2-6.5. Several destructive earthquakes also occurred in the Aceh Province, such as in Pidie Jaya in 2016 with Mw 6.5, which resulted in 101 fatalities and more than 800 people were injuries, as well as damage to various public infrastructures and the Takengon earthquake on July 2, 2013, which resulted in 30 people died.

Gravity data have been proven to be used to map subsurface fracture structures (Hiramatsu et al., 2019; Vos et al., 2006). However, for areas that are very large and difficult to access, the measurements are usually carried out by airplane, which requires a lot of funding and becomes an obstacle for developing countries. Fortunately, nowadays, there are free-access gravity satellite data with different resolutions, such as the GOCE and GRACE satellites with a resolution of 5 km/px (Rexer and Hirt, 2015), TOPEX/Poseidon satellite with a resolution of 1.3 km/px (Chatterjee et al., 2007; Yanis et al., 2021a), and Global Gravity Model plus (GGM+) data which combines GRACE, GOCE and EGM2008 data to obtain a high gravity data of 200 m/px (Hirt et al., 2013; Yanis et al., 2022). In this study, we processed the GGM+ data using 3D transformation and inversion to find correlations between seismicity data and fault structures in the central region of Aceh.

The application of gravity method has been successfully applied in several areas, such as for mapping fault structures in the Andaman Sea (Purnachandra Rao et al., 2011; Yanis et al., 2023), the Aceh and Seulimum segments (Yanis et al., 2021b), and it is even used to visualize local faults in the Geuredong volcano in the central part of Aceh and the geological structure on the Weh Island (Abdullah et al., 2022). In addition, satellite gravity data have been confirmed to have the same anomaly responses as Shipborne Gravity data over the Indian Offshore Regions (Chatterjee et al., 2007) and in Hudson Bay (Keating and Pinet, 2013). In the regional area, the global gravity data also has the potential to map the geological structure of the eastern Mediterranean region with its complex geology, so that it can be used as an important implication for tectonic-seismological analysis in the region (Eppelbaum and Katz., 2012, 2015).

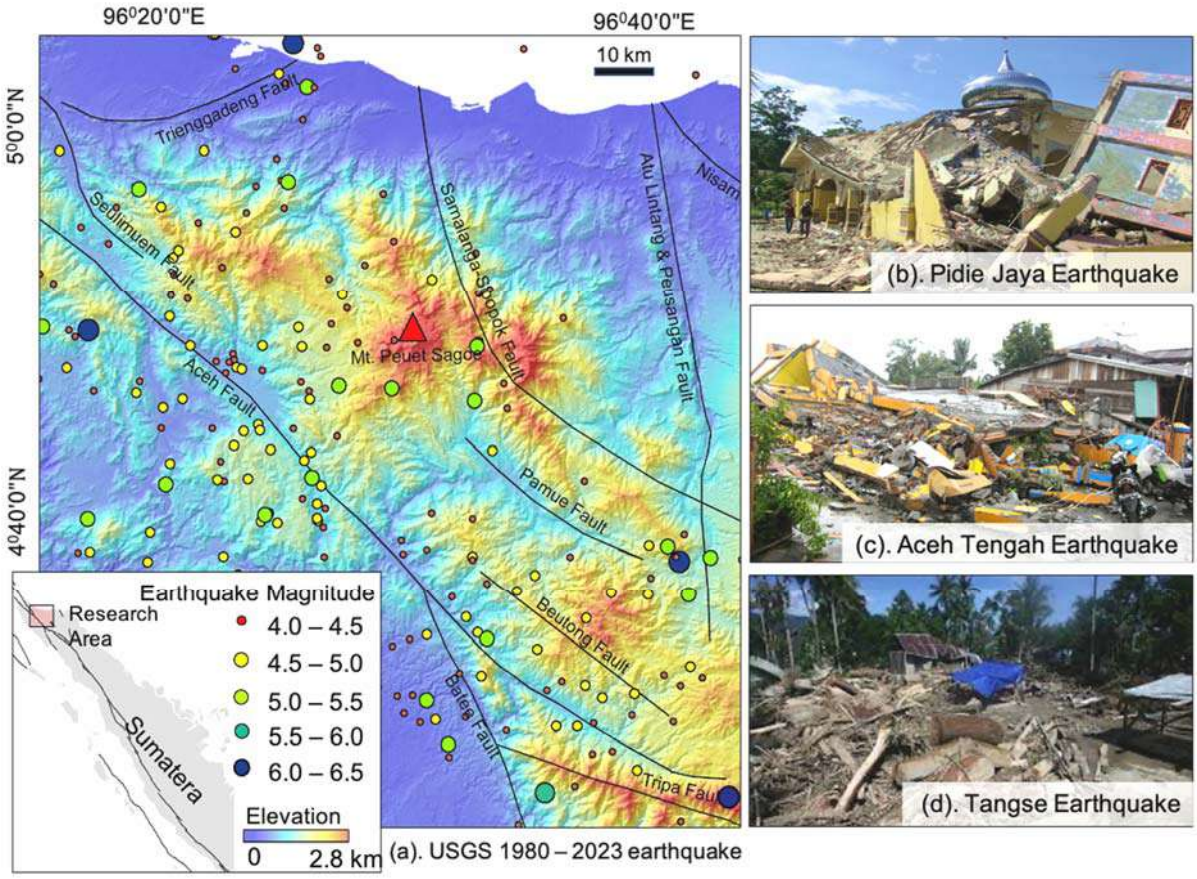

Fig. 1. (a) The distribution of earthquake magnitudes along with the Tringgadeng Segment to the Tripa Fault in the central part of Aceh from 1980-2023 obtained from the USGS, some of the damage caused by earthquakes that occurred along the Great Sumatran Fault such as (b) Pidie Jaya Earthquake on 6 December 2016, (c) Earthquake Central Aceh on Tuesday 2 July 2013, and (d) Tangse Earthquake which occurred on 22 December 2013

The data also shows a similar pattern to the ground gravity data (Yanis et al., 2021b; Yanis et al., 2023). These facts could make global gravity data, the main tool for studying geological structures on a global scale.

2. Geological and Tectonic Framework

The formation of geological structures in Aceh is generally influenced by tectonic activities from convergent forces of two plates, the Eurasian and Indo-Australian Plates, which form subduction zones along the Southwest of Sumatra Island (Bradley et al., 2017; Sieh and Natawidjaja, 2000; Yanis et al., 2023). As a result, it has produced a row of Bukit Barisan and GSF, which divides the island from the Andaman Sea to Semangko Bay. The GSF that transverses Aceh is divided into four main segments, the Aceh, Seulimuem, Tripa, and the Batee Segment, where the Aceh Segment stretches from the Central Aceh to the Aceh Island in a northwest-southeast direction for 200 km (Rizal et al., 2019; Ghosal et al., 2012; Sieh and Natawidjaja, 2000; Yanis et al., 2021b).

The Seulimuem Segment structure stretches for 120 km and continues to Weh Island in the northern part of Banda Aceh. This segment also passes the Seulawah Agam volcano in the southwest (Marwan et al., 2022; Marwan et al., 2021). The tectonic history of the Seulimuem Segment recorded earthquakes of Mw > 6.4 in 1936 and 1965 (Muksin et al., 2019; Sieh and Natawidjaja, 2000). The modified geological map (Fig, 2) shows that several rock formations, such as the Alluvium, Keutapang, Idi, Geumpang, Kluet, and Meulaboh formations dominate the study area. These rock formations are formed from various types of rocks, including intrusive and extrusive igneous rocks, clastic and non-clastic sedimentary rocks, and metamorphic rocks. Clastic sedimentary rocks dominate areas near the coast and lowlands, caused by weathering transported to those places.

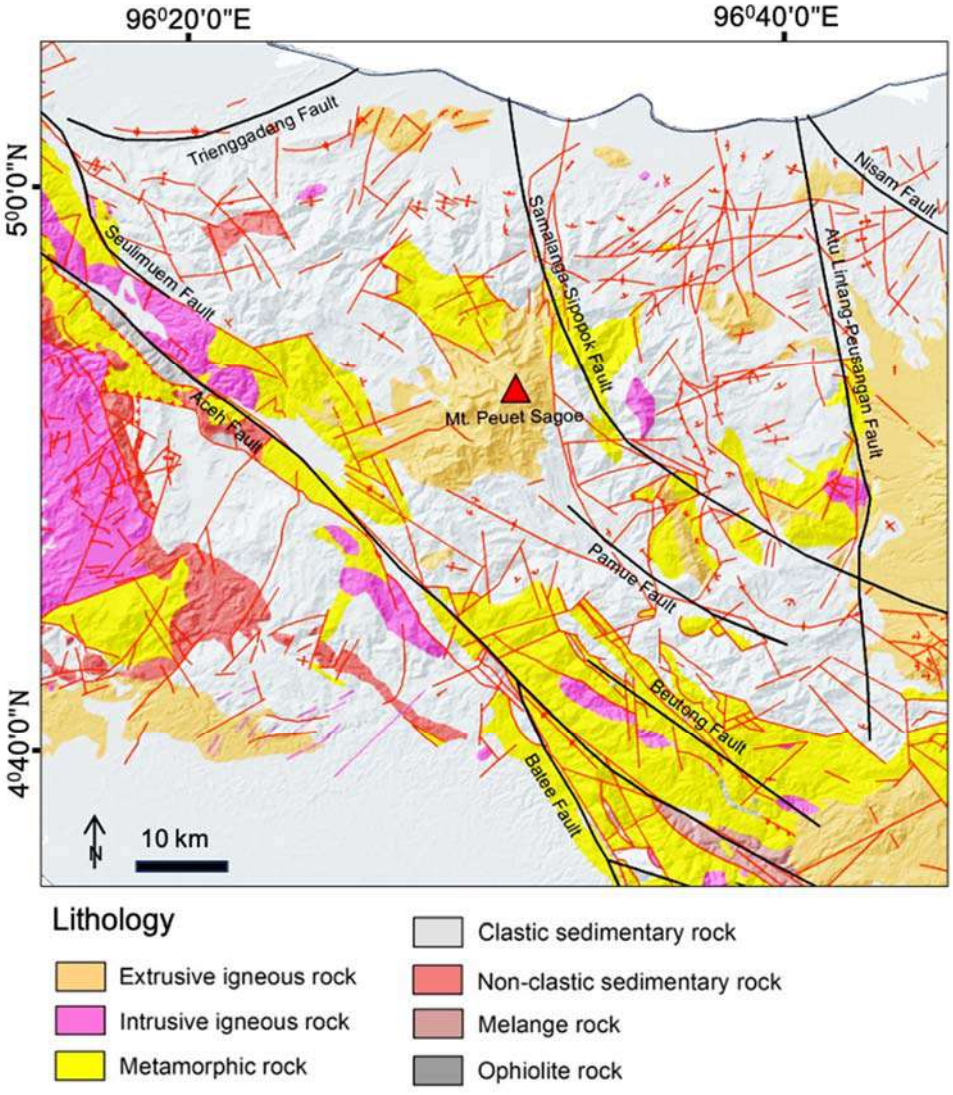

Fig. 2. A geological map shows the distribution of rocks dominated by metamorphic and igneous rock in the study area; the red line is the geological structure, while the black line is the GSF fracture from several segments

The research area also contains several fault segments of the GSF, such as the Tripa and Batee Segments. This area also has a significant role in seismic activity in Aceh, where there have been devastating earthquakes originating from the Tripa Segment with a magnitude of Mw 6.0 in 1990 and 1997. In addition, several other active faults spread across the central part of Aceh play a role in seismic activity. Tectonic activity in the subduction zone and the GSF line in Aceh has resulted in a high frequency of earthquakes. Since 2010-2023, there have been many earthquakes of various magnitudes. The strength of the earthquakes that occurred in that time interval was dominated by magnitudes Mw 4.0-5.0. In addition, several other earthquakes occurred with magnitudes Mw 5.1-7.8, and some were destructive, especially those at magnitudes Mw > 6.0 (Muzli et al., 2018; Muksin et al., 2018).

3. Theory and Data observation

3.1 Basic Theory of Gravity

The basic principle of the gravitational field is an attractive force that arises between two objects with masses as Newton's law of gravity states that the value is proportional to the multiplication of the masses and inversely proportional to the square of the distance between their centers of mass (Hinze et al., 2010). Many methods can be used to acquire gravity data, starting from marine, ground and airborne surveys, besides global observation data are freely available which is acquired using satellites (van der Meijde et al., 2015; Kern et al., 2003; Yanis et al., 2022). Satellite gravity data have been corrected for several parameters so that it is generally available in the free-air anomalies (Andersen and Knudsen, 2000; Dewanto et al., 2022). Currently, many satellites provide gravitational field data on the earth's surface, i.e. the European Space Agency, the ERS-1 satellite, and the Geodetic Satellite, which recorded gravitational field data above the earth's surface. Unfortunately, the resolution of the data is in the range of 2-25 km globally, so it is generally used for studies in large areas (Pavlis et al., 2012). In addition, there are also gravity field data, which have a high resolution of up to 200 m/px obtained from a combination of GRACE and GOCE satellite data, namely the Global Gravity Model Plus (GGM+) data, which have been widely used for various studies of geological structures in large and local areas.(Tassis et al., 2013; Yanis et al., 2022; Hirt et al., 2013; Chatterjee et al., 2007).

3.2 Global Gravity Model Plus (GGM+)

GGM+ is satellite gravitational field data obtained from the results of a combination of 3 satellites: GRACE, GOCE gravity satellites (spatial scale ~10,000 km to ~100 km), and EGM2008 (spatial scale ~100 km to ~10 km). In general, the GGM+ model data is calculated based on the following equation.

$$\left[\sum_{i=1}^{4}(A^T\Sigma(l)^{-1}A)_{GOCE,i} + (A^T\Sigma(l)^{-1}A)_{GRACE}\right]x = \left[\sum_{i=1}^{4}(A^T\Sigma(l)^{-1}l)_{GOCE,i} + (A^T\Sigma(l)^{-1}l)_{GRACE}\right] \quad (1)$$

where A is the Jacobian matrix, l is the observed value of gravity, and Σ is a form of realistic variances. The unknown spherical harmonic coefficient is represented as x. The GRACE calculation component consists of ITG-GRACE2010s data obtained based on GRACE's k-band spanning rates and kinematic orbit data in the 2002-2009 time interval.

3.3 Free Air Anomaly

GGM+ provides high-resolution data of 200 m/px, covering all land areas and can be accessed freely via http://ddfe.curtin.edu.au/gravitymodels/GGM+/. Several data types are obtained from GGM+, such as gravity disturbance, acceleration, North-South deflection, East-West deflection, and quasi-geoid height. Only the gravity disturbance data is equivalent to free-air anomaly data, which is used to interpret the geological structure of Central Aceh with an area of 111 km x 111 km. Figure 3 shows a comparison of the resolution between the available gravity data from several sources in the study area, where GGM+ data has 250,000 data points, Earth Gravitational Models (EGM) 2008 has 576 points, and World Gravity Map (WGM) 2012 has 961 data stations. Hence, the resolution from GGM+ is very good for studying geological structures in the local areas, as also found by (Hirt et al., 2014) and (Dewanto et al., 2022).

3.4 Enhancement Technique

Analysis of subsurface structures such as faults can be performed through gravity data transformation. For fault studies, data transformation is carried out through several types of derivative analysis, including the first horizontal derivative, a technique for filtering the gravity value for the first derivative of the horizontal plane. HD or horizontal gradient can be used to see changes in the rate of gravity values towards x and y directions in units of mGal/m, as shown in eq.2

$$HD\ (x,y) = \sqrt{\left(\frac{\partial \Delta g}{\partial x}\right)^2 + \left(\frac{\partial \Delta g}{\partial y}\right)^2} \quad (2)$$

Where $\frac{\partial \Delta g}{\partial x}$ and $\frac{\partial \Delta g}{\partial y}$ are the first derivative of the gravity anomaly in the x and y horizontal directions.

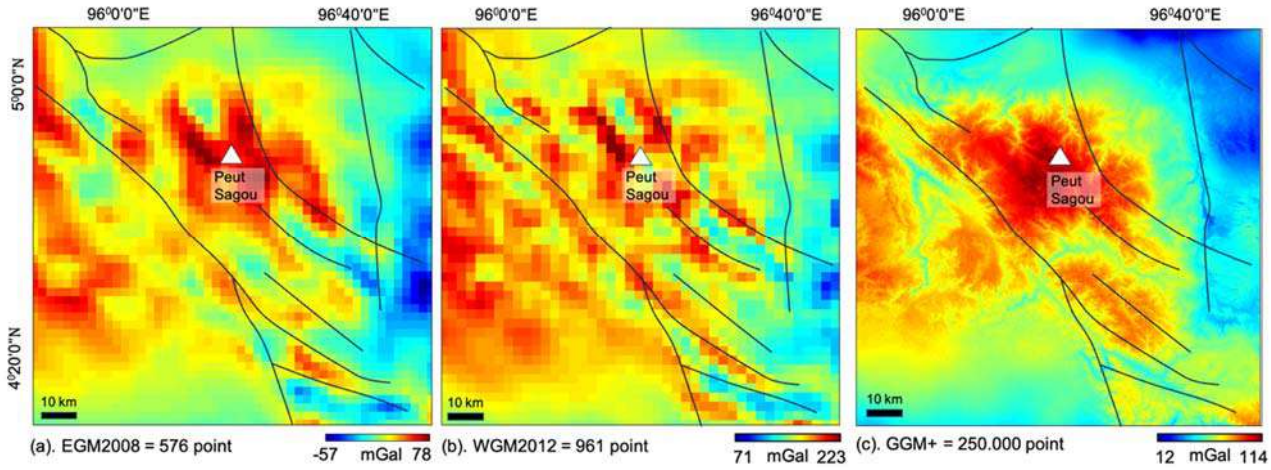

Fig. 3. Comparison of gravity anomaly from several satellite data with different resolutions in the research area, (a) Earth Gravitational Models (EGM) 2008 with a total of 576 points, (b) World Gravity Map (WGM) 2012 with 961 data points, and (c) GGM+ with a resolution of 200 m/px and 250,000 total data points

In addition, there is also a first vertical derivative method that calculates the first derivative in the vertical direction from the gravity data. The vertical derivative (VD) is mathematically calculated using the Laplace equation (Vaish and Pal, 2015).

$$VD = \frac{\partial^2 \Delta g}{\partial z^2} = -\left(\frac{\partial^2 \Delta g}{\partial x^2} + \frac{\partial^2 \Delta g}{\partial y^2}\right) \quad (3)$$

where Δg is the value of the gravity anomaly, x and y are the components of the horizontal direction, and z is the vertical direction component. A filter was also obtained by comparing the vertical plane derivative with the absolute amplitude of the total horizontal plane derivative, namely the tilt derivative. This filter can detect the boundaries of geological structures based on the angle obtained from comparing vertical and horizontal derivatives, which can be written mathematically (Doğru et al., 2017).

$$TDR = tan^{-1}\left(\frac{\frac{\partial^2 \Delta g}{\partial z^2}}{\sqrt{\left(\frac{\partial \Delta g}{\partial x}\right)^2 + \left(\frac{\partial \Delta g}{\partial y}\right)^2}}\right) \quad (4)$$

where $\frac{\partial \Delta g}{\partial z}$ is the vertical derivative in the z-direction.

4. Result and Interpretation

4.1 Bouguer Anomaly

To get the Bouguer anomaly, assuming the density that dominates the study area is necessary. The parameter is obtained from a geological map generally composed of alluvial clastic sedimentary rocks. The density value of this rock is in the range of 1.96-2.10 g/cm^3 with an average value of 2.05 g/cm^3. This average value is used in the calculation of the Bouguer correction. The results of the Bouguer anomaly were also overlaid with the fault structure obtained from several previous studies (Muksin et al., 2018; Sieh and Natawidjaja, 2000). After the Bouguer and terrain correction was made using the SRTM 30 m/px data, a complete Bouguer anomaly was obtained as shown in Fig. 4a, which varies between 12-114 mGal as a representative of the difference of rock density in the middle part of Aceh area. High Bouguer values (80-114 mGal) are found in the middle of the study area which is the response to high topography and the accumulation of densities in the form of intrusive igneous rocks from the Peut Sagoe Volcano. At the same time, the east and the south side areas are dominated by low Bouguer values (12-18 mGal), which are the response to the metamorphic rock density of the study area.

In some areas that are estimated to have regional faults, such as the Aceh and Seulimum Segments, the Bouguer data show the existence of the geological features through relatively low-value data that infiltrate high-value data. The pattern is also seen in the Pameu and Beutong Segments. However, the existence of other faults, such as the Tringgadeng Segment, which caused a 6.3 Mw earthquake in 2016, cannot be shown properly. The same things also happened in the Batee and Samalanga Segments. Therefore, we separated the residual and regional anomalies from the gravity data. The anomalies were separated using a cut-off wavelength of 50,000 m obtained from wave spectrum analysis through a Fourier transform (Pham et al., 2020). The residual anomalies were generated by applying high-pass filtering which allows high-frequency data representing near-surface anomalies as shown in Fig.4b.

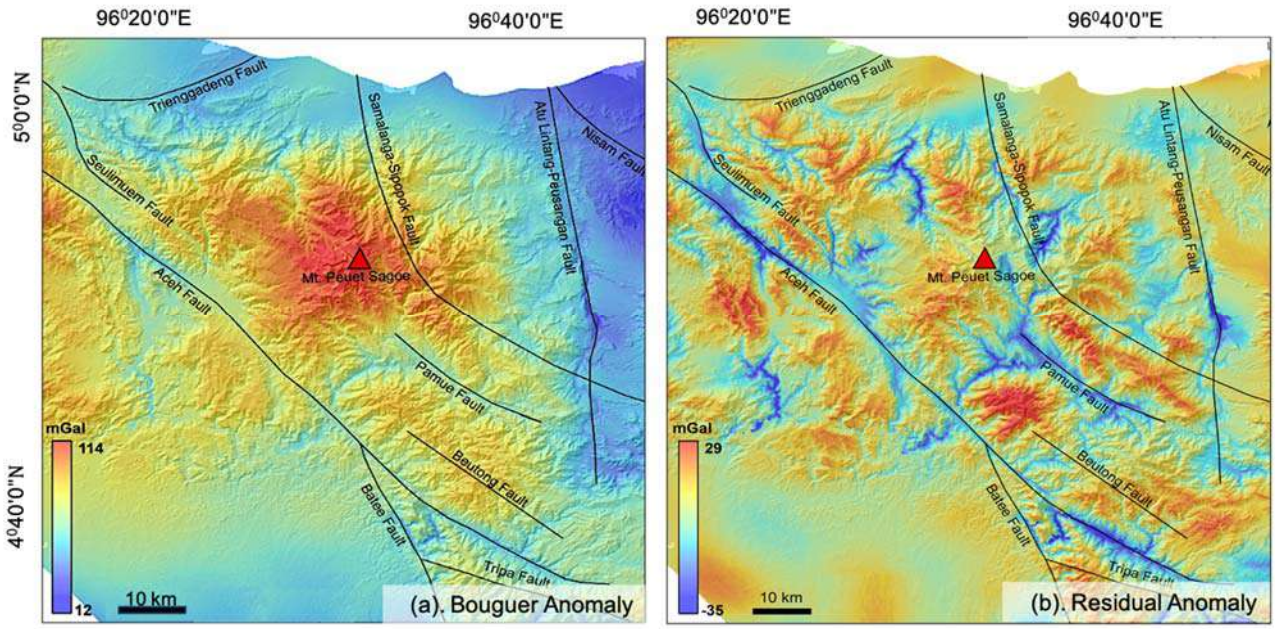

Fig. 4. (a) Complete Bouguer anomaly from GGM+ that was corrected for terrain using SRTM 30m/px data, high Bouguer values are found in the volcanic areas and several faults, while low Bouguer values dominate Tringgadeng dan Nissam Fault, while (b) is a residual anomaly from the Bouguer data indicating the presence of a fault in Central Aceh

The residual anomaly varies between -35 to 29 mGal, representing the subsurface density value from the local anomaly, where the high Bouguer value is no longer focused on the volcanic area but is evenly distributed in all places as a response to the geological features. Residual anomaly data can clearly show the existence of several faults generally characterized by low gravity values (-35 to 5 mGal), such as the Aceh Segment which runs straight from east to west of the study area. In addition, the residual anomaly data can reveal the existence of the Pameu Segment in the NW-SE direction which was previously not clear in the Bouguer anomaly. The same thing can also be seen in the Samalaga – Sipopok Segment, which is characterized by low and flanked by high anomalies. The existence of the Seulimum Segment in the NW-SE direction and the Alue Lintang-Peusangan Segment in the N-S direction, which caused significant seismic activity in Aceh Province, was also previously unclear in the Bouguer data. Still, the segments can be described clearly in the residual anomaly data. Although the residual values can show the existence of the faults, several faults still cannot be described properly, such as the Beutong Segment in the NW-SE direction and the Trienggadeng Segment in the SW-NE direction, which caused the 2016 earthquake in Pidie Jaya. Therefore, it is necessary to do some data enhancement using digital filtering to clarify the presence of subsurface geological features (Pham et al., 2020; Nasuti et al., 2012; Yanis et al., 2021a).

4.2 Derivative Anomaly

Qualitative interpretation techniques were used to clarify the existence of geological structures, such as the horizontal derivative (Fig.5a) which is the first derivative of the gravity data to its coordinates. According to Cooper (2006), fault structures and geological features from horizontal derivative results indicate areas flanked by high and low values side by side. The results of the first derivative in the horizontal direction vary between 0.045-5 mGal/m, where the low values are at the edge of the research area without geological structure (Bennett et al., 1981). Whereas in the middle area there are several faults dominated by high and low values which represent the existence of subsurface structures, such as the Aceh, Batee, Samalanga-Sipopok Segments and also the Alue Lintang-Peusangan Segment. The existence of these faults can be easily differentiated from the surrounding areas such as at the junction of three faults, The Batee, Tripa, and Aceh Segments indicated by high horizontal derivative values. However, other geological features, such as the Nisam Fault, cannot be mapped caused by slow tectonic motion. So that traces of these structures are not visible on the surface.

For that purpose, we clarify the existence of the features using another technique called tilt derivative which has a range of values from $-\pi/2$ to $\pi/2$ or -1.57 radian to 1.57 radian, as shown by Fig. 5b. where the tilt will be positive above the source of the anomaly, zero at the edge of the structure, and a negative value outside of the object. So the tech-

niques are very useful for simplicity in detecting the geological structures and the host area around the anomaly (Cooper and Cowan, 2006; Yanis et al., 2021b). Based on the tilt derivative data, it can be shown that 0 rad is the edge of the structure in an area where there are fault segments, such as the Batee Fault which is visible extending from the NW-SE direction, and the Aceh Segment which also intersects with the Batee Fault.

In addition, the Nisam Fault which previously could not be mapped by the horizontal filter, the tilt derivative can visualize the existence of the structure in the NW-SE direction which is characterized by high radian values. The same thing can be seen from the Pameu and Beutong Faults, which previously could not be mapped properly. As a complementary, the vertical derivative values were also calculated which only focused on several faults, especially for fault areas that cannot be described by the two previous filters, such as the western part (Fig. 5c) and the eastern (Fig. 5d) of the measurement location.

The vertical derivative anomaly in the vertical direction varies between -0.072 to 0.054 mGal/m. On the left side of the Trienggadeng Fault structure, the anomaly can be described well through the high derivative values which extend in the W-E direction, even though the existence of the fault that caused the Pidie Jaya Earthquake in 2016 is not visible on the surface. The same is also illustrated for the Seulimum Segment, which has significant seismic activity. The vertical anomaly can visualize a structure that extends in the NW-SE direction close to the Aceh Segment.

In the area between Trieggadeng and Seulimum Fault, several other high and low anomalies are suspected to be a response to local geological structures caused by the vertical derivative in meters. In the eastern part of the study area, the vertical derivative data can properly describe the existence of the Aceh Faults in the NW-SE direction, which is characterized by a low derivative value as a response to the edges of the subsurface anomaly structure. The same thing can be seen from the Batee Fault which is dominated by seismicity with 4.0-5.5 Mw, while at the Tripa and Beutong Segments the seismic activities are < 5 Mw which cannot be described from the previous filter. So, this vertical derivative can also show the existence of these faults with high values as a representation of the local structure from the other faults.

4.3 3D inversion model of Gravity

To obtain geological depth in the subsurface, such as faults, we carried out a 3D modelling by integrating the geological and seismicity data as the model's constraints. The 3D modelling was done using the GRABLOX 1.6 Software developed by (Pirttijarvi, 2008; Yanis et al., 2022; Yanis et al., 2023). In the calculation process, the Singular Value Decomposition (SVD) and Occam's Inversion were used to get the best density solution that correlates with the actual condition below the surface. The SVD algorithm decomposes a matrix into two matrices, while Occam's Inversion is an inversion method that utilizes the model's roughness level. Mathematically the density value from the inversion results is calculated using the following equation.

$$\Delta g\,(\boldsymbol{r}) = g_z\,(\boldsymbol{r}) = G\frac{\partial}{\partial_z}\int_v \frac{\rho(\boldsymbol{r}')}{|\boldsymbol{r}-\boldsymbol{r}|}dV' \qquad (5)$$

G is the gravity constant $\boldsymbol{r} = (x - x_0)\boldsymbol{i} + (y - y_0)\boldsymbol{j} + (z - z_0)\boldsymbol{k}$ that provide the vector position of the data measuring, r is a vector in volume V integration, and $\rho(r')$ is the volume of material density at the location V. The initial step in this inversion is determining the number of grids as model parameters, where the x and y axes are divided into 20 blocks (nx = 20, ny = 20) while the z-axis is ten blocks (nz = 10). The initial model length in the x and y directions is 111 km (dX = 30 km, dY = 111 km) with a model depth of 30 km (dZ = 30 km). This depth information was obtained from analysis of the USGS seismicity data from 1980-2023. So, the total number of blocks (N = nX x nY x nZ) is obtained as many as 4,000 blocks, and each block represents an area of 5.5 km for the x and y directions and 3 km for the z-direction. The selected background density is 2.67 gr/cc as a response to the average density in the earth's crust. Specifically, the optimal 3D gravity inversion models and blocks in the middle of the Aceh region are shown in Fig. 6. Using a computer powered by a Core i5 processor and 8 GB RAM capacity. It took about 25 hours to complete the inversion process, with 10 times the number of iterations needed to get the best model solution. The RMS data obtained from the inversion process was 5.21%.

The interpretation of the 3D model was carried out on the slice depth that cuts through the fault structure, as shown in Fig. 7 with a density range of 2-3 gr/cc. At a depth of 0 km (Fig. 7a), there are high-density values of 2-2.3 gr/cc spread in the middle, which is suspected as an intrusive igneous rock type associated with the volcanic activities of the Peut Sagoe volcano. The high-density values of 2.4-2.65 gr/cc are also found in the western part as a representative of extrusive igneous rocks such as rhyolite and andesite. However, low-density rocks dominate the Nisam, Beutong, and Tripa Faults on the east side. The seismic traces of the earthquakes in these areas are relatively small com-

pared to the Aceh and Seulimum Segments on the west side as it is known that each fault has its characteristics, including depth and geometry which greatly affect the impact of the damage caused. For example, the identified Trienggadeng Fault is at a depth of 3 km. The density data at 0 to 10 km can show this segment's existence, characterized by high-density values. Still, this structure cannot be visualized completely due to the sedimentation process on the surface.

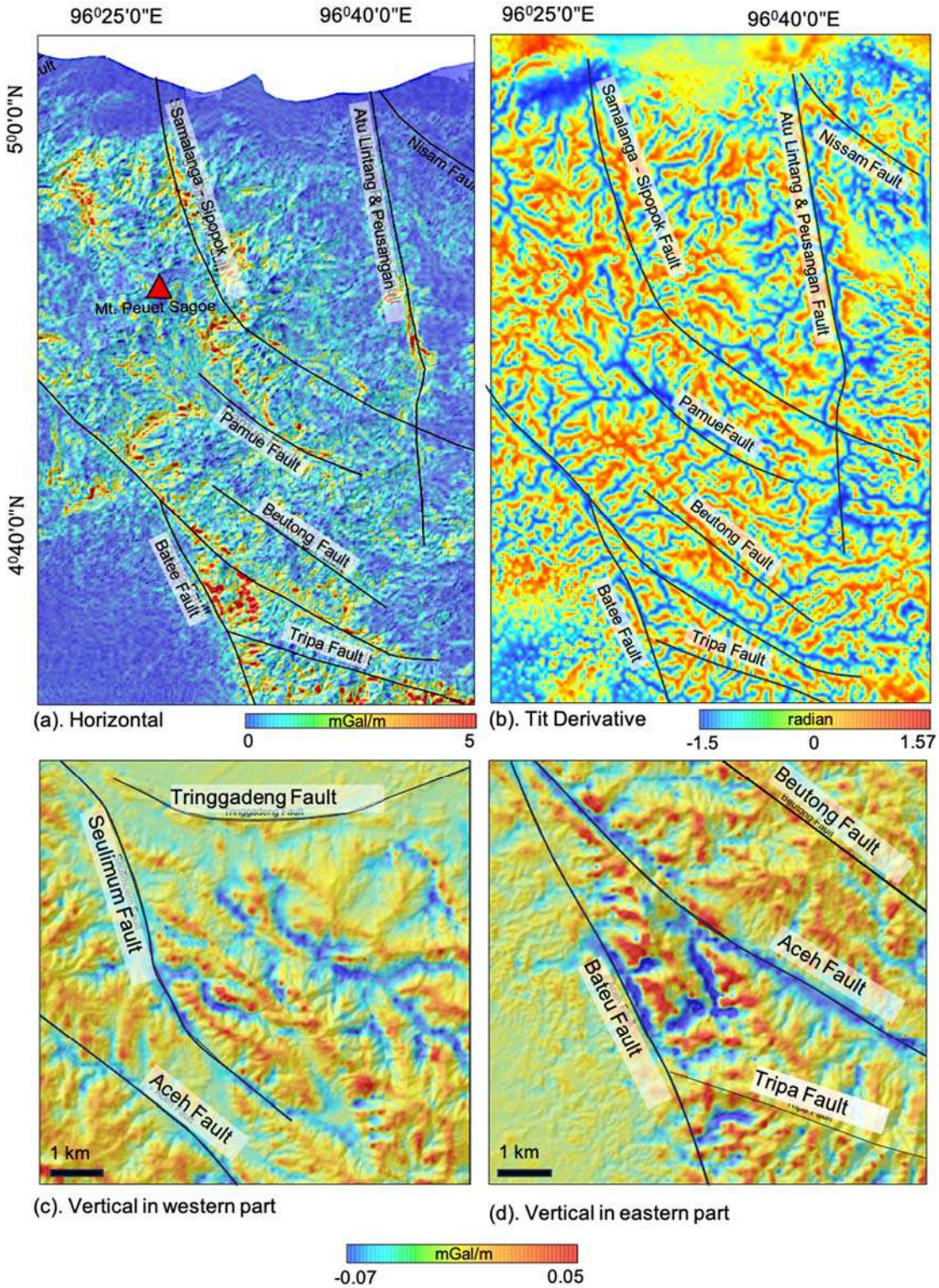

Fig. 5. The Bouguer data transformation clarifies the existence of geological structures below the surface. (a) Horizontal derivative, which is sensitive to horizontal changes, (b) Tilt derivative, while the vertical derivative is calculated for several highlight fault segments, such as in (c) the western region, which has the Trienggaden and Seulimum Segments, and (d) the eastern region which has the Bate and Aceh Segments

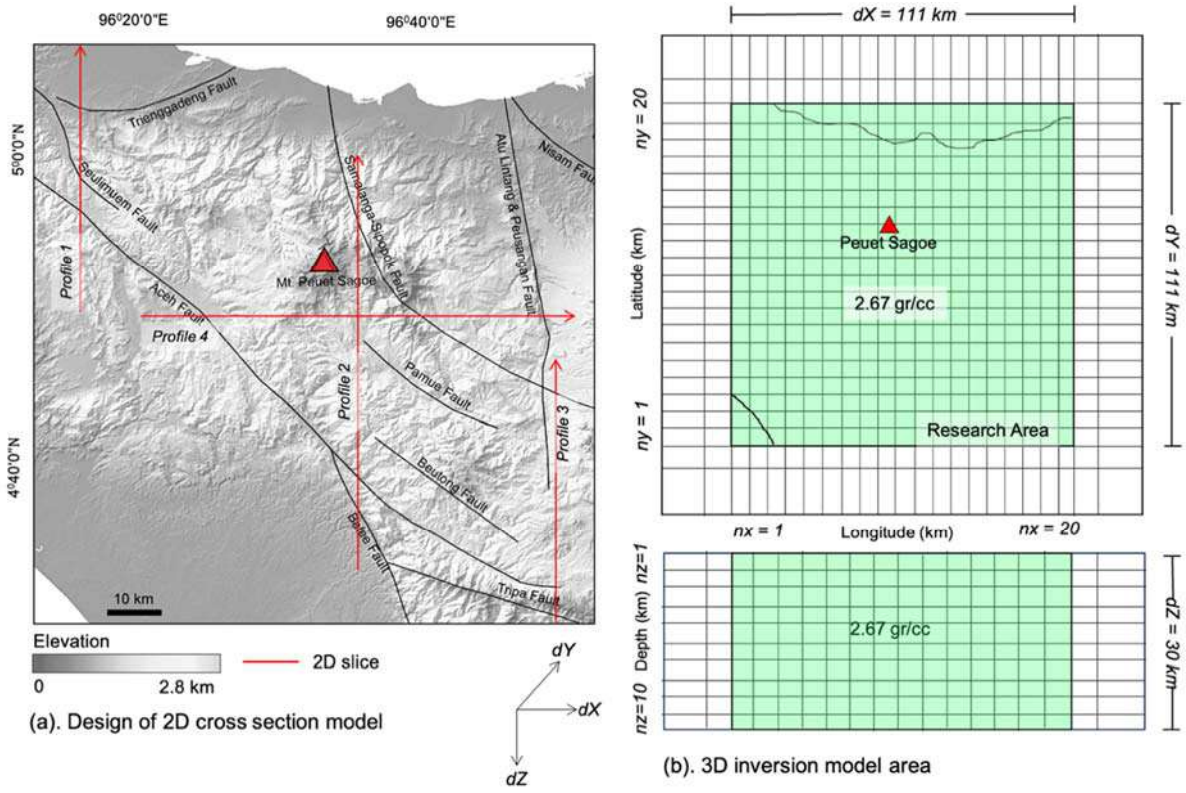

Fig. 6. Inversion of the 3D gravity data uses Occam and SVD algorithms. Where (a) designs a 2D cross-section model on several faults, while (b) is a 3D inversion model that shows a matrix of values nx and ny = 20, while nz 10 represents the subsurface depth

In addition, the Aceh and Seulimum Segments in the NW-SE direction can be described well through high-density and low-density values of the Lintang – Peusangan Fault on the east side of the measurement location. At a depth of 10 km (Fig. 7b), the whole Trienggadeng Segment can still be shown well, stretching in the W-E direction with high-density values. At this depth, the medium-density values dominate the measurement area and indicate several faults below the surface, such as the Aceh Segment on the west side and the Pameu and Beutong Segments with low-density values on the east side. At depths of 10 km (Fig. 7c) and 15 km (Fig. 7d), the anomalies generally show the same pattern; for example the high-density values are focused on the Samalanga-Sipopok Segment area in response to the subsurface metamorphic rocks, where the density models at this depth are still able to show the presence of faults with significant traces of seismic activities such as the Seulimum and Aceh Segments which extended in the NW-SE direction, the Tripa, Pameu, and Trienggadeng Segments with low seismic activities. Overall, the 3D anomaly model can show the rock density of the geological structures in the Central Aceh region. Still, this model is not very sensitive to map residual structures such as the Nisam Fault, which has relatively few seismic activities.

4.4 2D cross-section model

A 2D cross-section model was also created from the 3D gravity inversion to study the depth and geometry of the faults. There are four 2D profiles sliced intersecting several faults in the northern region of Aceh Province. For instance, Profile 1 (Fig. 8a) shows contrasting rock densities at 0-30 km depths. At a distance of 25 km from the profile, the presence of the Aceh Fault can be demonstrated at a depth of 8 km below the surface, characterized by high-density values and proofed by significant seismic activity. In addition, the Trienggadeng Fault can also be shown by a high density at the same depth as the Aceh Segment. Meanwhile, the Seulimum Segment, which is 30 km from the profile, is characterised by a low-density value extending from the surface to 25 km below the surface.

In Profile 2 (Fig. 8b), the existence of the Aceh Segment on the east side is also shown at a depth of 8 km with high density which correlates with Profile 1. The Batee Segment in the N-W direction also shows high density and is connected with the Aceh Segment on the east side. At the same time, the Samalanga-Sipopok Segment in the NW-SE direction can also be mapped at a depth of 8 km. In general, the presence of the subsurface faults is indicated by contrast differences in high-density data as shown in Profile 3 (Fig. 8c) as shown in the Samalanga-Sipopok Segment at a distance of 25-50 km and the Tripa Segment at a distance of 0-20 km.

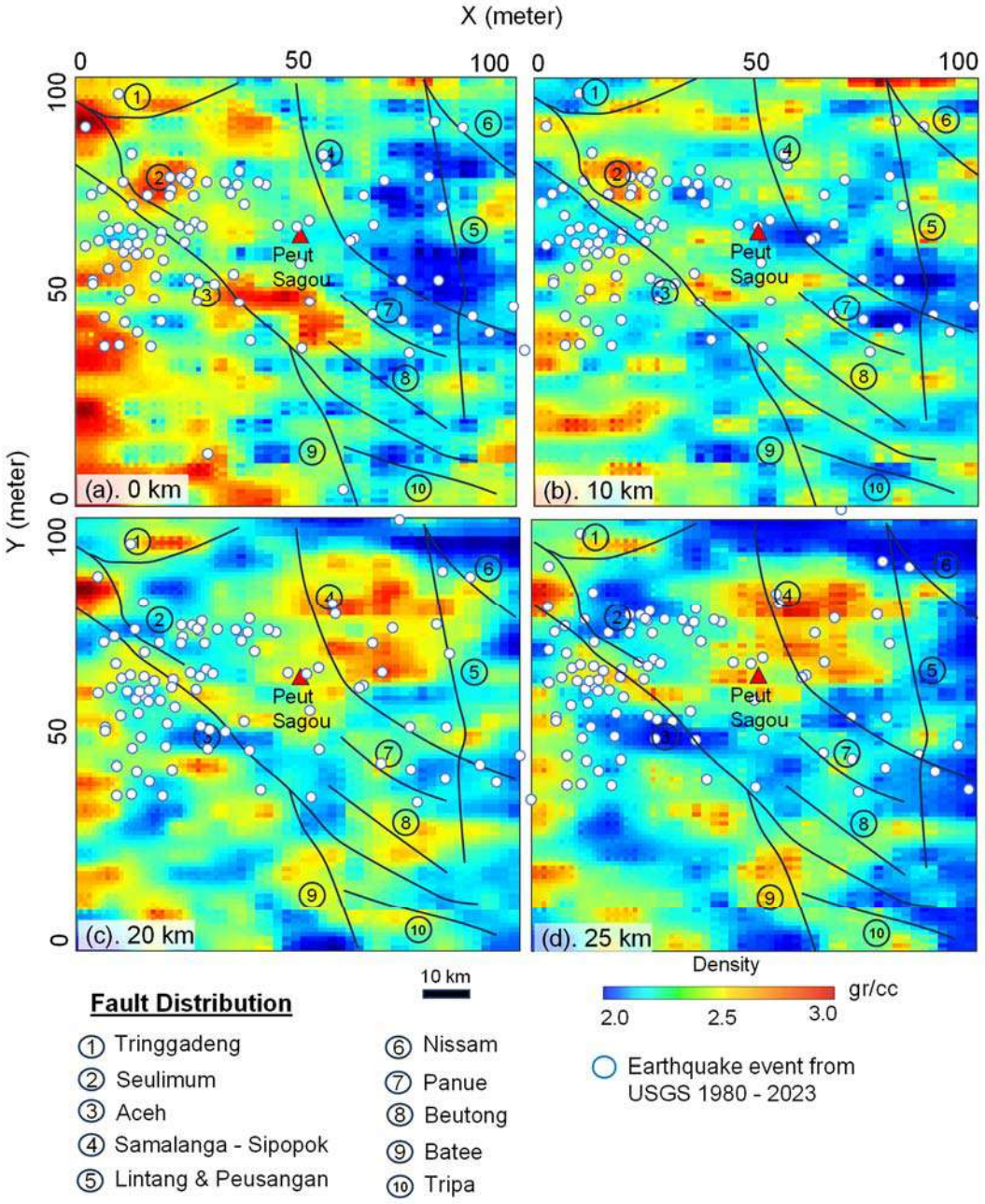

Fig. 7. The 3D slice model shows the distribution of density with depths of (a) 0 km, (b) 10 km, (c) 20 km, and (d) 25 km, which indicate the presence of a rock with a density of 2 – 3 gr/cc

This cross-sectional model can show the subsurface fault geometry. However, several faults cannot be visualized properly, such as in Profile 4 (Fig. 8d), where the rock density is unable to show the existence of the Aceh and Samalanga-Sipopok Segments instead the rock density contrast represents a weak zone that may intersect with the presence of faults.

5. Conclusion

Earthquake disaster mitigation must be done as early as possible to minimise material losses and casualties. So far, the studies on faults in Aceh Province have only focused on the Aceh and Seulimum Segments, while the North of Aceh region has yet to be studied. Even though the location also has several fault segments that can cause earthquakes. This study discusses the efficiency of the GGM+ global gravity data with a resolution of 200 m/px for mapping the geological structure in Central Aceh, which has several fault segments and many seismic activities. The approaches described here included the Bouguer anomaly, digital transformation, 2D modelling, and also 3D modelling of gravity. Based on the data analyses, the existence of a fault structure can be indicated by Bouguer anomaly of -35 to 5 mGal, such as the Seulimum Segment in the NW-SW direction and Alue Lintang – Peusangan in the N-S direction.

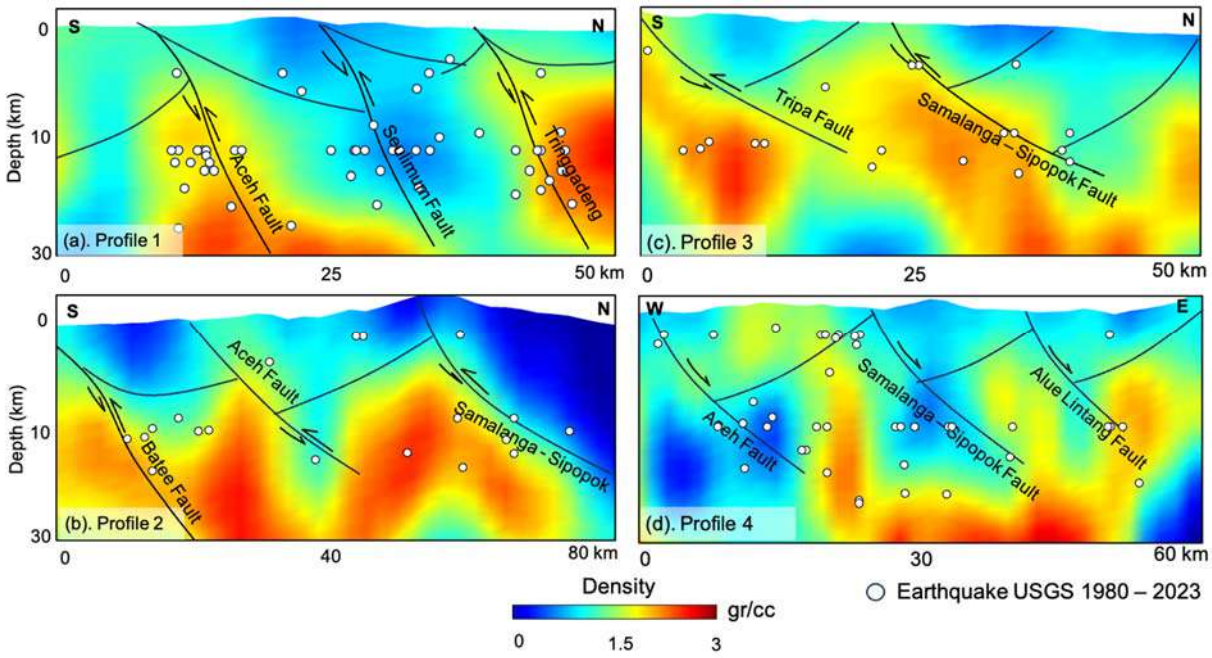

Fig. 8. The 2D cross-section model that was overlaid with the earthquake epicenter from the USGS and the interpretation of the presence of faults from the geological map, (a) Profile 1 which is traversed by several segments such as the Aceh, Seulimum, and Trienggadeng Faults, (b) Profile 2 which intersects the Samalanga-Sipopok Segment, (c) Profile 3 in Tripa Fault area, and (d) Profile 4 in the Alue Lintang Fault area. The density contrast of the inverted 3D gravity data can visualize the presence of these faults

In contrast, the existence of the Batee Fault, Tripa, and Aceh Segments can be clarified through high horizontal derivative anomaly (> 2 mGal/m). In addition, we also applied vertical derivative and tilt derivative filters to clarify structures that cannot be mapped from the previous filter, where the results obtained can clearly show the existence of the Trienggadeng Segment in the W-E direction, the Batee Segment and the Aceh Fault in NW-SE direction. The results of the 3D modelling combined with seismicity and geology data as the data constraints can show the depth of the faults in the Central Aceh region at 8 km below the surface, where the geometry of several segments such as the Aceh, Samalanga, and Trienggadeng Faults can be visualized with a density of 1.8 gr/cc as a representation of intrusive igneous rocks in the research area. GGM+ data analyses have been successfully used as a rapid and low-cost method for mapping fault structures correlated with seismic activity. It can be used as an initial stage in analysing fault presence in various other locations, especially in tropical countries with high topography where mobilising survey instruments is very difficult.

6. Acknowledgement

We are very grateful to the students of Geophysical Engineering at Universitas Syiah Kuala, especially Jhordi Saputra, who helped a lot in processing and modelling the gravity observation data. We also thank Marrku Pittijarvi, who developed the Grablox 10.6 software for 3D gravity modelling.

Funding

Data collection and article writing were funded by a Lektor Research Grant of Universitas Syiah Kuala, which was given to Muhammad Yanis with contract No. 279/UN11.2.1/PT.01.03/PNBP/2023.

REFERENCES

Abdullah F. et al. Subsurface mapping of fault structure in the Weh island by using a 3D density of global gravity. GEOMATE Journal, Vol. 23, No. 96, 2022, pp. 121-128.

Andersen O.B. and Knudsen P. The role of satellite altimetry in gravity field modelling in coastal areas. Physics and Chemistry of the Earth, Part A: Solid Earth and Geodesy, Vol. 25, No. 1, 2000, pp. 17-24, DOI:10.1016/S1464-1895(00)00004-1.

Bennett J.D. et al. The geology of the Banda Aceh Quadrangle, Sumatra. Geological Research and Development Center, Bandung. Explanatory Note. 1981, 19 p.

Bradley K.E. et al. Implications of the diffuse deformation of the Indian Ocean lithosphere for slip partitioning of oblique

ЛИТЕРАТУРА

Abdullah F. et al. Subsurface mapping of fault structure in the Weh island by using a 3D density of global gravity. GEOMATE Journal, Vol. 23, No. 96, 2022, pp. 121-128.

Andersen O.B. and Knudsen P. The role of satellite altimetry in gravity field modelling in coastal areas. Physics and Chemistry of the Earth, Part A: Solid Earth and Geodesy, Vol. 25, No. 1, 2000, pp. 17-24, DOI:10.1016/S1464-1895(00)00004-1.

Bennett J.D. et al. The geology of the Banda Aceh Quadrangle, Sumatra. Geological Research and Development Center, Bandung. Explanatory Note. 1981, 19 p.

Bradley K.E. et al. Implications of the diffuse deformation of the Indian Ocean lithosphere for slip partitioning of oblique

plate convergence in Sumatra. Journal of Geophysical Research: Solid Earth, Vol. 122, No. 1, John Wiley and Sons Ltd. Jan. 2017, pp. 572-591, DOI:10.1002/2016JB013549.

Chatterjee S. et al. Validation of ERS-1 and high-resolution satellite gravity with in-Situ Shipborne gravity over the Indian Offshore Regions: Accuracies and implications to subsurface modeling. Marine Geodesy, Vol. 30, No. 3, Aug. 2007, pp. 197-216, DOI:10.1080/01490410701438323.

Cooper G.R.J. Interpreting potential field data using continuous wavelet transforms of their horizontal derivatives. Computers and Geosciences, Vol. 32, 2006, pp. 984-992, DOI:10.1016/ j.cageo.2005.10.012.

Cooper G.R.J. and Cowan D.R. Enhancing potential field data using filters based on the local phase. Computers and Geosciences, Vol. 32, No. 10, 2006, pp. 1585-1591, DOI:10.1016/ j.cageo.2006.02.016.

Dewanto B.G. et al. The 2022 Mw 6.1 Pasaman Barat, Indonesia earthquake, confirmed the existence of the Talamau segment fault based on teleseismic and satellite gravity data. Quaternary, Vol. 5, No. 4, p. 45, 2022, DOI:10.3390/quat5040045.

Doğru F. et al. Application of tilt angle method to the Bouguer gravity data of Western Anatolia. Bulletin of the mineral research and exploration, 2017, Vol. 155, No. 155, pp. 213-222.

Eppelbaum L.V. and Katz Y.I. Key features of seismoneotectonic pattern of the Eastern Mediterranean. Proceedings of National acad. Sci. Azerb. Rep., Ser.: The Sciences of Earth, No. 3, 2012, pp. 29-40.

Eppelbaum L.V. and Katz, Yu.I. Newly developed paleomagnetic map of the Easternmost Mediterranean Joined with tectono-structural analysis Unmask geodynamic history of this region. Central European Jour. of Geosciences (Open Geosciences), Vol. 7, No. 1, 2015, pp. 95-117.

Ghosal D. et al. New insights on the offshore extension of the Great Sumatran fault, NW Sumatra, from marine geophysical studies. Geochemistry, Geophysics, Geosystems, Vol. 13, No.11, 2012, DOI:10.1029/2012GC004122.

Hill E.M. et al. The 2012 Mw 8.6 Wharton Basin sequence: A cascade of great earthquakes generated by near-orthogonal, young, oceanic mantle faults. Journal of Geophysical Research: Solid Earth, Vol. 120, No. 5, John Wiley and Sons Ltd. 2015, pp. 3723-3747, DOI:10.1002/2014JB011703.

Hinze W.J. et al. Gravity and magnetic exploration: principles, practices, and applications. cambridge university press, Jan. 2010, 512 p., DOI:10.1017/CBO9780511843129.

Hiramatsu Y. et al. Gravity gradient tensor analysis to an active fault: a case study at the Togi-Gawa Nangan fault, Noto Peninsula, Central Japan. Earth, Planets and Space, Vol. 71, No. 1, Springer. Berlin, Heidelberg, 2019, DOI:10.1186/s40623-019-1088-5.

Hirt C., Claessens S. et al. New ultrahigh-resolution picture of Earth's gravity field. Geophysical Research Letters, Vol. 40, No. 16, Aug. 2013, pp. 4279-4283, DOI:10.1002/grl.50838.

Hirt C., Kuhn M. et al. Study of the Earth's short-scale gravity field using the ERTM2160 gravity model. Computers and Geosciences, Vol. 73, Elsevier, 2014, pp. 71-80, DOI:10.1016/ j.cageo.2014.09.001.

Ito T. et al. Isolating along-strike variations in the depth extent of shallow creep and fault locking on the Northern Great Sumatran Fault. Journal of Geophysical Research, Vol. 117, No. B6, 2012, pp. 1-16, DOI:10.1029/2011JB008940.

Keating P. and Pinet N. Comparison of surface and shipborne gravity data with satellite-altimeter gravity data in Hudson Bay. The Leading Edge, Society of Exploration Geophysicists, Vol. 32, No. 4, 2013, pp. 450-458, https://doi.org/ 10.1190/tle32040450.1.

Kern M. et al. A Study on the combination of satellite, airborne and terrestrial gravity data. Journal of Geodesy, Vol. 77, pp. 217-225, 2003, DOI:10.1007/s00190-003-0313-x.

plate convergence in Sumatra. Journal of Geophysical Research: Solid Earth, Vol. 122, No. 1, John Wiley and Sons Ltd. Jan. 2017, pp. 572-591, DOI:10.1002/2016JB013549.

Chatterjee S. et al. Validation of ERS-1 and high-resolution satellite gravity with in-Situ Shipborne gravity over the Indian Offshore Regions: Accuracies and implications to subsurface modeling. Marine Geodesy, Vol. 30, No. 3, Aug. 2007, pp. 197-216, DOI:10.1080/01490410701438323.

Cooper G.R.J. Interpreting potential field data using continuous wavelet transforms of their horizontal derivatives. Computers and Geosciences, Vol. 32, 2006, pp. 984-992, DOI:10.1016/ j.cageo.2005.10.012.

Cooper G.R.J. and Cowan D.R. Enhancing potential field data using filters based on the local phase. Computers and Geosciences, Vol. 32, No. 10, 2006, pp. 1585-1591, DOI:10.1016/ j.cageo.2006.02.016.

Dewanto B.G. et al. The 2022 Mw 6.1 Pasaman Barat, Indonesia earthquake, confirmed the existence of the Talamau segment fault based on teleseismic and satellite gravity data. Quaternary, Vol. 5, No. 4, p. 45, 2022, DOI:10.3390/quat5040045.

Doğru F. et al. Application of tilt angle method to the Bouguer gravity data of Western Anatolia. Bulletin of the mineral research and exploration, 2017, Vol. 155 No. 155, pp. 213-222.

Eppelbaum L.V. and Katz Y.I. Key features of seismoneotectonic pattern of the Eastern Mediterranean. Proceedings of National acad. Sci. Azerb. Rep., Ser.: The Sciences of Earth, No. 3, 2012, pp. 29-40.

Eppelbaum L.V. and Katz, Yu.I. Newly developed paleomagnetic map of the Easternmost Mediterranean Joined with tectono-structural analysis Unmask geodynamic history of this region. Central European Jour. of Geosciences (Open Geosciences), Vol. 7, No. 1, 2015, pp. 95-117.

Ghosal D. et al. New insights on the offshore extension of the Great Sumatran fault, NW Sumatra, from marine geophysical studies. Geochemistry, Geophysics, Geosystems, Vol. 13, No.11, 2012, DOI:10.1029/2012GC004122.

Hill E.M. et al. The 2012 Mw 8.6 Wharton Basin sequence: A cascade of great earthquakes generated by near-orthogonal, young, oceanic mantle faults. Journal of Geophysical Research: Solid Earth, Vol. 120, No. 5, John Wiley and Sons Ltd. 2015, pp. 3723-3747, DOI:10.1002/2014JB011703.

Hinze W.J. et al. Gravity and magnetic exploration: principles, practices, and applications. cambridge university press, Jan. 2010, 512 p., DOI:10.1017/CBO9780511843129.

Hiramatsu Y. et al. Gravity gradient tensor analysis to an active fault: a case study at the Togi-Gawa Nangan fault, Noto Peninsula, Central Japan. Earth, Planets and Space, Vol. 71, No. 1, Springer. Berlin, Heidelberg, 2019, DOI:10.1186/s40623-019-1088-5.

Hirt C., Claessens S. et al. New ultrahigh-resolution picture of Earth's gravity field. Geophysical Research Letters, Vol. 40, No. 16, Aug. 2013, pp. 4279-4283, DOI:10.1002/grl.50838.

Hirt C., Kuhn M. et al. Study of the Earth's short-scale gravity field using the ERTM2160 gravity model. Computers and Geosciences, Vol. 73, Elsevier, 2014, pp. 71-80, DOI:10.1016/ j.cageo.2014.09.001.

Ito T. et al. Isolating along-strike variations in the depth extent of shallow creep and fault locking on the Northern Great Sumatran Fault. Journal of Geophysical Research, Vol. 117, No. B6, 2012, pp. 1-16, DOI:10.1029/2011JB008940.

Keating P. and Pinet N. Comparison of surface and shipborne gravity data with satellite-altimeter gravity data in Hudson Bay. The Leading Edge, Society of Exploration Geophysicists, Vol. 32, No. 4, 2013, pp. 450-458, https://doi.org/ 10.1190/tle32040450.1.

Kern M. et al. A Study on the combination of satellite, airborne and terrestrial gravity data. Journal of Geodesy, Vol. 77, pp. 217-225, 2003, DOI:10.1007/s00190-003-0313-x.

Lay T. et al. The Great Sumatra-Andaman earthquake of 26 December 2004. Science, Vol. 308, No. 5725, American Association for the Advancement of Science, May 2005, pp. 1127-33, DOI:10.1126/SCIENCE.1112250.

Marwan M. et al. A low-cost UAV based application for identify and mapping a geothermal feature in Ie Jue Manifestation, Seulawah Volcano, Indonesia. International Journal of GEOMATE, Vol. 20, No. 80, 2021, pp. 135-142, DOI:10.21660/2021.80.J2044.

Marwan M. et al. geoelectrical model of geothermal spring in Ie Jue Seulawah deriving from 2D VLF-EM and DC resistivity methods. Journal of Applied Engineering Science, Vol. 21, No. 1, 2023, pp.59-69, DOI:10.5937/JAES0-38014.

McCaffrey R. The Tectonic Framework of the Sumatran Subduction Zone. Annual Reviews, Vol. 37, Apr. 2009, pp. 345-366, DOI:10.1146/annurev.earth.031208.100212.

Muksin U. et al. Investigation of Aceh Segment and Seulimeum Fault by using seismological data; A preliminary result. Journal of Physics: Conference Series, Vol. 1011, No. 1, Apr. 2018, p. 012031, DOI:10.1088/1742-6596/1011/1/012031.

Muksin U. et al. AcehSeis Project provides insights into the detailed seismicity distribution and relation to fault structures in Central Aceh, Northern Sumatra. Journal of Asian Earth Sciences, Vol. 171, 2019, pp. 20-27, Elsevier, DOI:10.1016/J.JSEAES.2018.11.002.

Muzli M. et al. The 2016 Mw 6.5 Pidie Jaya, Aceh, North Sumatra, earthquake: Reactivation of an unidentified sinistral fault in a region of distributed deformation. Seismological Research Letter, Vol. 89, No. 5, 2018, pp. 1761-1772, DOI:10.1785/0220180068.

Nasuti A. et al. Onshore-offshore potential field analysis of the Møre-Trøndelag fault complex and adjacent structures of Mid Norway. Tectonophysics, Vol. 518-521, 20 January 2012, pp. 17-28, DOI:10.1016/J.TECTO.2011.11.003.

Natawidjaja D.H. and Triyoso W. The Sumatran fault zone – from source to hazard. Journal of arthquake and Tsunami, Vol. 1, No. 01, World Scientific, 2007, pp. 21-47.

Pavlis N.K. et al. The development and evaluation of the earth gravitational model 2008 (EGM2008). Journal of Geophysical Research: Solid Earth, Vol. 117, No. 4, 2012, pp. 1-38, DOI:10.1029/2011JB008916.

Pham L.T. et al. Enhancement of potential field source boundaries using an improved logistic filter. Pure and Applied Geophysics, Vol. 177, No. 11, 2020, pp. 5237-5249, DOI:10.1007/s00024-020-02542-9.

Pham L.T. et al. Subsurface structural mapping from high-resolution gravity data using advanced processing methods. Journal of King Saud University, Science, Vol. 33, No. 5, 2021, p. 101488, DOI:10.1016/j.jksus.2021.101488.

Pirttijarvi M. Gravity interpretation and modeling software based on 3-D block models. GRABLOX. User's Guide to Version, 2008.

Purnachandra Rao N. et al. Structure and tectonics of the Andaman Subduction Zone from modeling of seismological and gravity data. In: New Frontiers in Tectonic Research - General Problems, Sedimentary Basins and Island Arcs, Intech Publisher/ Rijeka, Croatia, 2011, DOI:10.5772/19090.

Rexer M. and Hirt Ch. Spectral analysis of the Earth's topographic potential via 2D-DFT: A new data-based degree variance model to degree 90,000. Journal of Geodesy, Vol. 89, No. 9, Sept. 2015, pp. 887-909, DOI:10.1007/s00190-015-0822-4.

Rizal M. et al. The 2D resistivity modelling on north sumatran fault structure by using magnetotelluric data. IOP Conference Series: Earth and Environmental Science, Vol. 364, Dec. 2019, p. 012036, DOI:10.1088/1755-1315/364/1/012036.

Sieh K. and Natawidjaja D. Neotectonics of the Sumatran Fault, Indonesia. Journal of Geophysical Research: Solid Earth,

Lay T. et al. The Great Sumatra-Andaman earthquake of 26 December 2004. Science, Vol. 308, No. 5725, American Association for the Advancement of Science, May 2005, pp. 1127-33, DOI:10.1126/SCIENCE.1112250.

Marwan M. et al. A low-cost UAV based application for identify and mapping a geothermal feature in Ie Jue Manifestation, Seulawah Volcano, Indonesia. International Journal of GEOMATE, Vol. 20, No. 80, 2021, pp. 135-142, DOI:10.21660/2021.80.J2044.

Marwan M. et al. geoelectrical model of geothermal spring in Ie Jue Seulawah deriving from 2D VLF-EM and DC resistivity methods. Journal of Applied Engineering Science, Vol. 21, No. 1, 2023, pp.59-69, DOI:10.5937/JAES0-38014.

McCaffrey R. The Tectonic Framework of the Sumatran Subduction Zone. Annual Reviews, Vol. 37, Apr. 2009, pp. 345-366, DOI:10.1146/annurev.earth.031208.100212.

Muksin U. et al. Investigation of Aceh Segment and Seulimeum Fault by using seismological data; A preliminary result. Journal of Physics: Conference Series, Vol. 1011, No. 1, Apr. 2018, p. 012031, DOI:10.1088/1742-6596/1011/1/012031.

Muksin U. et al. AcehSeis Project provides insights into the detailed seismicity distribution and relation to fault structures in Central Aceh, Northern Sumatra. Journal of Asian Earth Sciences, Vol. 171, 2019, pp. 20-27, Elsevier, DOI:10.1016/J.JSEAES.2018.11.002.

Muzli M. et al. The 2016 Mw 6.5 Pidie Jaya, Aceh, North Sumatra, earthquake: Reactivation of an unidentified sinistral fault in a region of distributed deformation. Seismological Research Letter, Vol. 89, No. 5, 2018, pp. 1761-1772, DOI:10.1785/0220180068.

Nasuti A. et al. Onshore-offshore potential field analysis of the Møre-Trøndelag fault complex and adjacent structures of Mid Norway. Tectonophysics, Vol. 518-521, 20 January 2012, pp. 17-28, DOI:10.1016/J.TECTO.2011.11.003.

Natawidjaja D.H. and Triyoso W. The Sumatran fault zone – from source to hazard. Journal of arthquake and Tsunami, Vol. 1, No. 01, World Scientific, 2007, pp. 21-47.

Pavlis N.K. et al. The development and evaluation of the earth gravitational model 2008 (EGM2008). Journal of Geophysical Research: Solid Earth, Vol. 117, No. 4, 2012, pp. 1-38, DOI:10.1029/2011JB008916.

Pham L.T. et al. Enhancement of potential field source boundaries using an improved logistic filter. Pure and Applied Geophysics, Vol. 177, No. 11, 2020, pp. 5237-5249, DOI:10.1007/s00024-020-02542-9.

Pham L.T. et al. Subsurface structural mapping from high-resolution gravity data using advanced processing methods. Journal of King Saud University, Science, Vol. 33, No. 5, 2021, p. 101488, DOI:10.1016/j.jksus.2021.101488.

Pirttijarvi M. Gravity interpretation and modeling software based on 3-D block models. GRABLOX. User's Guide to Version, 2008.

Purnachandra Rao N. et al. Structure and tectonics of the Andaman Subduction Zone from modeling of seismological and gravity data. In: New Frontiers in Tectonic Research - General Problems, Sedimentary Basins and Island Arcs, Intech Publisher/ Rijeka, Croatia, 2011, DOI:10.5772/19090.

Rexer M. and Hirt Ch. Spectral analysis of the Earth's topographic potential via 2D-DFT: A new data-based degree variance model to degree 90,000. Journal of Geodesy, Vol. 89, No. 9, Sept. 2015, pp. 887-909, DOI:10.1007/s00190-015-0822-4.

Rizal M. et al. The 2D resistivity modelling on north sumatran fault structure by using magnetotelluric data. IOP Conference Series: Earth and Environmental Science, Vol. 364, Dec. 2019, p. 012036, DOI:10.1088/1755-1315/364/1/012036.

Sieh K. and Natawidjaja D. Neotectonics of the Sumatran Fault, Indonesia. Journal of Geophysical Research: Solid Earth,

Vol. 105, No. B12, 2000, pp. 28295-28326, DOI:10.1029/ 2000jb900120.
Tassis G.A. et al. A new Bouguer gravity anomaly field for the Adriatic Sea and its application for the study of the crustal and upper Mantle Structure. Journal of Geodynamics, Vol. 66, 2013, pp. 38-52, Elsevier, DOI:10.1016/j.jog.2012.12.006.
Vaish J. and Pal S.K. Geological mapping of Jharia Coalfield , India using GRACE EGM2008 gravity data: A vertical derivative approach. Geocarto International, Vol. 30, No. 4, 2015, pp. 388-401, DOI:10.1080/10106049.2014.905637.
van der Meijde M. et al. GOCE data, models and applications: A review. International Journal of Applied Earth Observation and Geoinformation, Vol. 35, Part A, March 2015, pp.4-15, DOI:10.1016/j.jag.2013.10.001.
Vos I.M.A. et al. Resolving the nature and geometry of major fault systems from geophysical and structural analysis: The Palmerville Fault in NE Queensland, Australia. Journal of Structural Geology,Vol. 28, No.11, November 2006, pp. 2097-2108, DOI:10.1016/j.jsg.2006.07.016.
Yanis M., Simanjuntak A.V.H., Abdullah F. et al. Application of Seismicity and Gravity Observation-Based Filtering Model for Mapping a Fault Structure in Weh Island, Indonesia. Iraqi Geology Journal, Vol. 56, July.2024, pp. 260–274. DOI:10.46717/IGJ.56.2A.20MS-2023-7-29.
Yanis M., Marwan M. et al. A pilot survey for mapping the fault structure around the Geuredong volcano by using high-resolution global gravity. Acta Geophysica, Vol.70, July 2022, pp.2057-2075, Springer, DOI:10.1007/S11600-022-00860-1.
Yanis M., Marwan M. et al. Application of GEOSAT and ERS Satellite as an Alternative method of gravity ground measurement in hydrocarbon basin in East Island. Indonesian Journal of Geography, Vol. 33, No. 2, Feb. 2020, DOI:10.22146/ mgi.50782 (in Indonesian).
Yanis M., Faisal A., Yenny A. et al. Continuity of Great Sumatran Fault in the marine area revealed by 3D inversion of gravity data. Jurnal Teknologi, Vol. 83, No. 1, Jan.2021, pp. 145-155, DOI:10.11113/jurnalteknologi.v83.14824.
Yanis M., Faisal A., Zaini N. et al. The northernmost part of the Great Sumatran Fault Map and images derived from gravity anomaly. Acta Geophysica, Vol. 69, No. 3, June 2021, pp. 795-807, DOI:10.1007/s11600-021-00567-9.

Vol. 105, No. B12, 2000, pp. 28295-28326, DOI:10.1029/ 2000jb900120.
Tassis G.A. et al. A new Bouguer gravity anomaly field for the Adriatic Sea and its application for the study of the crustal and upper Mantle Structure. Journal of Geodynamics, Vol. 66, 2013, pp. 38-52, Elsevier, DOI:10.1016/j.jog.2012.12.006.
Vaish J. and Pal S.K. Geological mapping of Jharia Coalfield , India using GRACE EGM2008 gravity data: A vertical derivative approach. Geocarto International, Vol. 30, No. 4, 2015, pp. 388-401, DOI:10.1080/10106049.2014.905637.
van der Meijde M. et al. GOCE data, models and applications: A review. International Journal of Applied Earth Observation and Geoinformation, Vol. 35, Part A, March 2015, pp.4-15, DOI:10.1016/j.jag.2013.10.001.
Vos I.M.A. et al. Resolving the nature and geometry of major fault systems from geophysical and structural analysis: The Palmerville Fault in NE Queensland, Australia. Journal of Structural Geology,Vol. 28, No.11, November 2006, pp. 2097-2108, DOI:10.1016/j.jsg.2006.07.016.
Yanis M, Simanjuntak A.V.H., Abdullah F. et al. Application of Seismicity and Gravity Observation-Based Filtering Model for Mapping a Fault Structure in Weh Island, Indonesia. Iraqi Geology Journal, Vol. 56, July.2024, pp. 260–274. DOI:10.46717/IGJ.56.2A.20MS-2023-7-29.
Yanis M., Marwan M. et al. A pilot survey for mapping the fault structure around the Geuredong volcano by using high-resolution global gravity. Acta Geophysica, Vol.70, July 2022, pp.2057-2075, Springer, DOI:10.1007/S11600-022-00860-1.
Yanis M., Marwan M. et al. Application of GEOSAT and ERS Satellite as an Alternative method of gravity ground measurement in hydrocarbon basin in East Island. Indonesian Journal of Geography, Vol. 33, No. 2, Feb. 2020, DOI:10.22146/ mgi.50782.
Yanis M., Abdullah F., YennyA. et al. Continuity of Great Sumatran Fault in the marine area revealed by 3D inversion of gravity data. Jurnal Teknologi, Vol. 83, No. 1, Jan.2021, pp. 145-155, DOI:10.11113/jurnalteknologi.v83.14824.
Yanis M., Abdullah F., Zaini N. et al. The northernmost part of the Great Sumatran Fault Map and images derived from gravity anomaly. Acta Geophysica, Vol. 69, No. 3, June 2021, pp. 795-807, DOI:10.1007/s11600-021-00567-9.

ИСПОЛЬЗОВАНИЕ ГЛОБАЛЬНОЙ ГРАВИТАЦИИ ДЛЯ КАРТИРОВАНИЯ СВЯЗИ МЕЖДУ СЕЙСМИЧНОСТЬЮ И ГЕОЛОГИЧЕСКИМ СТРОЕНИЕМ В СРЕДНЕЙ ЧАСТИ ПРОВИНЦИИ АЧЕХ, ИНДОНЕЗИЯ

Янис М.[1], Абдулла Ф.[1,2], Ананда Р.[3], Сямсюдин Ф.[1,2], Исмаил Н.[1,2], Зайнал М.[1], Паембонан А.Я.[4]

[1]Геофизический инженерный факультет, Университет Сийя Куала
Банда-Ачех 23111, Индонезия: yanis@usk.ac.id
[2]Физический факультет, Университет Syiah Kuala
Банда Ачех 23111, Индонезия
[3]Кафедра геофизической инженерии, Бандунгский технологический институт
Бандунг 40132, Индонезия
[4]Геофизический инженерный факультет, Технологический институт Суматры
Южный Лампунг 35365, Индонезия

Резюме. Ачех – одна из индонезийских провинций, подверженных землетрясениям, поскольку ее пересекают Большой Суматрский разлом и зоны субдукции вдоль западного побережья с высокой сейсмической активностью. В последнее время исследования по картированию разломов были сосредоточены на сегментах Ачех и Сеулимум в западной части провинции Ачех. В отличие от этого, центральная часть еще не изучена, несмотря на то, что за последние 10 лет произошло несколько землетрясений в районах, где трассы разломов все еще нуждаются в надлежащем картировании. Поэтому в данном исследовании использовалась глобальная гравитационная модель Plus (GGM+) с высоким разрешением 200 м/пкс для анализа взаимосвязи между сейсмичностью и структурами разломов в центральной части Ачеха. Остаточная аномалия GGM+ указывает на существование геологических структур, таких как сегменты Ачех, Памеу и Самаланга, характеризующихся низкой гравитацией. Для уточнения наличия разломов также применялись некоторые производные методы, например, горизонтальная производная аномалия для картирования сегментов Ачех, Бати, Самаланга и Алуэ Линтанг - Пеусанган. Вертикальная производная показывает существование разлома Трингаденг, предположительно являющегося источником землетрясения Пи-

ди Джая в 2016 году. Таким образом, производная наклона может также визуализировать наличие разлома Ниссам, что не отображается в других методах фильтрации. Мы также провели 3D гравитационное моделирование с использованием алгоритма Occam и сингулярного разложения; плотность указывает на глубину и геометрию структуры разлома, в целом 8 км, что обеспечивает надежность GGM+ при изучении разломов, особенно в высокогорных районах, где использование приборов затруднено.

Ключевые слова: *Гравитация, разлом, GGM +, провинция Ачех, геологическое строение, 3D инверсия*

İNDONEZİYANIN AÇEH ƏYALƏTİNİN ORTA HİSSƏSİNİN SEYSMİKLİK VƏ GEOLOJİ QURULUŞU ARASINDAKI ƏLAQƏNİ XƏRİTƏLƏNDİRMƏK ÜÇÜN QLOBAL CAZİBƏ QÜVVƏSİNDƏN İSTİFADƏ

Yanis M.[1] , Abdulla F.[1,2], Ananda R.[3], Səmsyudin F.[1,2] , İsmayıl H.[1,2], Zaynal M.[1], Paembonan A.Ya.[4]

[1]Geofizika mühəndislik fakültəsi, Sia Kuala Universiteti
Banda-Açeh 23111, İndoneziya: yanis@usk.ac.id
[2]Fizika fakültəsi, Syiah Kuala Universiteti
Banda-Açeh 23111, İndoneziya
[3]Geofiziki mühəndislik kafedrası, Bandunq texnologiya institutu
Bandunq 40132, İndoneziya
[4]Geofiziki mühəndislik fakültəsi, Sumatra texnologiya institutu
Cənubi Lampunq 35365, İndoneziya

Xülasə: Açeh - Böyük Sumatra fay xəttinin və yüksək seysmik aktivliyə malik, qərb sahili boyunca subduksiya zonalarının kəsişdiyi, zəlzələlərə məruz qalan Indoneziyanın vilayətlərindən biridir. Son zamanlar fay xətlərinin xəritələnməsi ilə bağlı tədqiqatlar Açeh vilayətinin qərb hissəsindəki Açeh və Seulimum seqmentlərinə fokuslanmışdır. Bununla yanaşı, son 10 ildə fay xətlərinin düzgün xəritələnməsinə ehtiyacı olan bölgələrdə bir neçə zəlzələ baş verməsinə baxmayaraq, mərkəzi hissə hələ də öyrənilməmişdir. Buna görə də, bu tədqiqatda Açehin mərkəzi hissəsində seysmik aktivlik ilə fay strukturları arasındakı əlaqəni təhlil etmək üçün 200 m/piks yüksək həllediciliklə Qlobal Qravitasiya Modeli Plus (GGM+) istifadə edilmişdir. GGM+ qalıq anomaliyası Açeh, Pameu və Samalanga seqmentləri kimi aşağı qravitasiya ilə səciyyələnən geoloji strukturların mövcudluğunu göstərir. Fayların varlığını dəqiqləşdirmək məqsədilə Açeh, Bati, Samalanga və Alue Lintang – Peusangan seqmentlərinin xəritələnməsi üçün üfüqi törəmə anomaliyası kimi bəzi törəmə metodları da tətbiq edilmişdir. Şaquli törəmə Tringgadeng qırılmasının mövcudluğunu göstərir, bu qırılma 2016-cı ildəki Pidie Jaya zəlzələsinin mənbəyi hesab olunur. Beləliklə, maillik törəməsi Nissam qırılmasının da mövcudluğunu vizuallaşdıra bilər, bu isə digər filtrləmə metodlarında görünmür. Biz həmçinin Occam alqoritmi və sinqulyar parçalanma metodundan istifadə edərək 3D cazibə modelləşdirilməsi apardıq; sıxlıq qırılmanın dərinliyini və strukturunu göstərir, ümumilikdə 8 km dərinliyindədir ki, bu da GGM+ metodunun etibarlılığını təmin edir, xüsusən də cihazların istifadəsinin çətin olduğu dağlıq ərazilərdə qırılmaların öyrənilməsində.

Açar sözlər*: Qravitasiya, qırılma, GGM +, Açex əyaləti, geoloji quruluş, 3D inversiya*